

# Evolutionary Paths of the cAMP-Dependent Protein Kinase (PKA) Catalytic Subunits

Kristoffer Søberg<sup>1,2</sup>, Tore Jahnsen<sup>2</sup>, Torbjørn Rognes<sup>3,4</sup>, Bjørn S. Skålhegg<sup>1</sup>, Jon K. Laerdahl<sup>4,5\*</sup>

**1** Department of Nutrition, Institute of Basic Medical Sciences, University of Oslo, Oslo, Norway, **2** Department of Biochemistry, Institute of Basic Medical Sciences, University of Oslo, Oslo, Norway, **3** Department of Informatics, University of Oslo, Oslo, Norway, **4** Centre for Molecular Biology and Neuroscience (CMBN), Department of Microbiology, Oslo University Hospital Rikshospitalet, Oslo, Norway, **5** Bioinformatics Core Facility, Department of Informatics, University of Oslo, Oslo, Norway

## Abstract

3',5'-cyclic adenosine monophosphate (cAMP) dependent protein kinase or protein kinase A (PKA) has served as a prototype for the large family of protein kinases that are crucially important for signal transduction in eukaryotic cells. The PKA catalytic subunits C $\alpha$  and C $\beta$ , encoded by the two genes *PRKACA* and *PRKACB*, respectively, are among the best understood and characterized human kinases. Here we have studied the evolution of this gene family in chordates, arthropods, mollusks and other animals employing probabilistic methods and show that C $\alpha$  and C $\beta$  arose by duplication of an ancestral PKA catalytic subunit in a common ancestor of vertebrates. The two genes have subsequently been duplicated in teleost fishes. The evolution of the *PRKACG* retroposon in simians was also investigated. Although the degree of sequence conservation in the PKA C $\alpha$ /C $\beta$  kinase family is exceptionally high, a small set of signature residues defining C $\alpha$  and C $\beta$  subfamilies were identified. These conserved residues might be important for functions that are unique to the C $\alpha$  or C $\beta$  clades. This study also provides a good example of a seemingly simple phylogenetic problem which, due to a very high degree of sequence conservation and corresponding weak phylogenetic signals, combined with problematic nonphylogenetic signals, is nontrivial for state-of-the-art probabilistic phylogenetic methods.

**Citation:** Søberg K, Jahnsen T, Rognes T, Skålhegg BS, Laerdahl JK (2013) Evolutionary Paths of the cAMP-Dependent Protein Kinase (PKA) Catalytic Subunits. PLoS ONE 8(4): e60935. doi:10.1371/journal.pone.0060935

**Editor:** Narayanaswamy Srinivasan, Indian Institute of Science, India

**Received:** December 12, 2012; **Accepted:** March 5, 2013; **Published:** April 12, 2013

**Copyright:** © 2013 Søberg et al. This is an open-access article distributed under the terms of the Creative Commons Attribution License, which permits unrestricted use, distribution, and reproduction in any medium, provided the original author and source are credited.

**Funding:** The project was funded by the Research Council of Norway. The funder had no role in study design, data collection and analysis, decision to publish, or preparation of the manuscript.

**Competing Interests:** The authors have declared that no competing interests exist.

\* E-mail: j.k.laerdahl@medisin.uio.no

## Introduction

Protein kinases are enzymes that catalyze the transfer of a phosphate group from adenosine 5'-triphosphate (ATP) to a serine, threonine, tyrosine or other residue on a substrate. Most eukaryotic protein kinases derive from a common ancestor kinase, and share the same core catalytic domain [1].

PKA (EC 2.7.11.11) is a serine/threonine kinase which is ubiquitously expressed in the human body. It is involved in many intracellular signaling events, and its function, specificity, and downstream effects depend on factors such as subcellular localization, expression of a number of isoforms and physiochemical features [2,3]. The inactive form of PKA is a heterotetrameric holoenzyme consisting of a regulatory (R) subunit dimer binding to two catalytic (C) subunits [4]. During activation, cAMP binds cooperatively to two sites termed A and B on each R subunit. In the inactive holoenzyme, only the B site is exposed and available for cAMP binding. When occupied, this enhances the binding of cAMP to the A site which leads to an intramolecular conformational change and the release of the R subunit dimer. The two C monomers are then free to phosphorylate relevant C substrates in the cytosol and nucleus [5–7]. Thus, a major function of the R subunit is to inhibit the phosphotransferase activity of the C subunits through direct interactions.

Several variants of the C and R subunits have been identified in human cells. Four R subunits designated RI $\alpha$ , RI $\beta$ , RII $\alpha$ , and RII $\beta$  are transcribed from separate genes [8]. PKA holoenzymes

containing RI and RII subunits are designated PKA type I and II, respectively [9,10]. Protein-protein interactions and organization of signal transduction pathways is required to obtain specificity in space and time. Protein kinases are localized to the relevant subcellular sites through anchoring, scaffolding and adapter protein activity. Major organizers of the cAMP signaling pathway are the A kinase anchoring proteins (AKAPs), which both function as scaffolding proteins and attach PKA to subcellular structures [11,12]. Initially, AKAPs were shown to interact with the RII subunits [13]. Later, dual specific AKAPs binding both RII and RI, as well as AKAPs binding only RI, have been identified, demonstrating that both PKA type I and II may be tethered to subcellular compartments in the cell [14–16].

Five different human C subunit genes have been identified; *PRKACA*, *PRKACB*, *PRKACG*, *PRKX*, and *PRKY* [2,17–19], all within the AGC group of kinases, which contains the cyclic-nucleotide-dependent family (PKA and PKG), the protein kinase C family, the  $\beta$ -adrenergic receptor kinase, the ribosomal S6 family and some other relatives of these kinases [1,20]. Three of the human C subunit genes, *PRKACA*, *PRKACB*, and *PRKX*, have been demonstrated to be transcribed and translated into functional protein kinases, termed PKA C $\alpha$ , PKA C $\beta$ , and PRKX, respectively. C $\alpha$  exhibits two splice variants, C $\alpha$ 1 [21] and C $\alpha$ 2 [22–24], by employing two alternative 5' exons in *PRKACA* (Fig. 1A). Whereas C $\alpha$ 1 is ubiquitously expressed in man, C $\alpha$ 2 is exclusively expressed in the sperm cell and has been shown to be

essential for sperm motility and fertilization [24–27]. A number of isoforms of human *PRKACB* have been identified with alternative splicing of exons 5' of exon 2 (Fig. 1A), encoding at least the following proteins: C $\beta$ 1, C $\beta$ 2, C $\beta$ 3, C $\beta$ 4, C $\beta$ 3ab, C $\beta$ 3b, C $\beta$ 3abc, C $\beta$ 4ab, C $\beta$ 4b, and C $\beta$ 4abc [28–33]. In addition, C $\beta$  variants formed by skipping of exon 4 are expressed in the brain of higher primates. These C subunits bind the R subunit in a cAMP-independent fashion [34].

PRKX, which is a protein kinase encoded from the X-chromosome, also binds RI $\alpha$  in a cAMP sensitive fashion [19]. PRKX and PRKY are 94% identical and have unknown functions [18,20]. *PRKACG* is a retroposon lacking introns and may be a pseudogene [35]. Whereas mRNA from *PRKACG* is solely, but ubiquitously, transcribed in the testis [17], the corresponding protein C $\gamma$  has never been identified. *In vitro* experiments on expressed C $\gamma$  have revealed a functional kinase with variant-specific properties. The C $\gamma$  protein kinase is, in contrast to C $\alpha$ , and most probably C $\beta$ , not inhibited by the Protein Kinase Inhibitor (PKI), and it requires higher concentrations of cAMP for dissociation from PKA type I holoenzymes [36,37]. The *in vivo* function of PKA C $\gamma$ , if the protein exists, remains to be elucidated.

The *PRKACA* and *PRKACB* genes share identical positions and intron phases for all nine introns, and are very likely the result of a gene duplication event (Fig. 1B). Human PKA C $\alpha$ 1 and C $\beta$ 1 have the same length (350 residues) and share 93% sequence identity. Many studies have elucidated the importance and function of a number of residues and short sequence segments in these kinases, and some of these are briefly summarized in Fig. 1C. The sequence identity between human PKA C $\alpha$  vs. C $\gamma$  and PRKX is, 82% and 54%, respectively, and between C $\alpha$ /C $\beta$  and other human kinases below 50%. PKA C kinases in invertebrate metazoa have sequence identity with human C $\alpha$ /C $\beta$  above 77% (see below), confirming that the PKA C $\alpha$ /C $\beta$ -like kinases, not including PRKX, builds a unique and compact clade/family of kinases within the AGC-group.

A previous study explored the evolution of the R subunits of PKA [38]. Based on a multiple sequence alignment (MSA) of the most conserved region in the R subunit sequences, the phosphate-binding cassette, the authors proposed a new classification of the R subunits in place of a classification based on physiochemical properties. They also identified a signature sequence that characterizes the R subunit genes, and identified type- and subtype-specific residues. The same focused analysis of the C subunits of PKA is to our knowledge lacking. In order to get a comprehensive overview of all the known PKA genes and obtain insight into the essential residues of these proteins, we have collected, compared and performed an extensive analysis of PKA C subunit sequences from a large number of bilaterian animal species. The homologous genes *PRKACA* and *PRKACB* constitute a unique clade of kinases and their protein products are the main sources of PKA activity in the cell. Therefore, we focused our analysis on the C $\alpha$ /C $\beta$ -like kinases, including C $\gamma$ , but not the more remotely related kinases PRKX and PRKY. The main focus of this study has been on elucidating the phylogeny of vertebrate and other chordate PKA C $\alpha$ /C $\beta$  homologs, while orthologous sequences from mollusks and arthropods were included mainly to serve as outgroups in the phylogenetic analysis. We show that an ancestor C subunit was duplicated around the time of the evolution of the first vertebrate species, giving rise to the paralogous genes encoding C $\alpha$  and C $\beta$ . Further analysis on the C $\alpha$ /C $\beta$  homologs revealed signature sequences characteristic of the two paralogs. Comparison of C $\alpha$  and C $\beta$  sequences gave insight into molecular differences and possible mechanisms that

may determine functional differences between these two prototype protein kinases.

## Materials and Methods

### Sequences of PKA C $\alpha$ /C $\beta$ Homologs

Homologous sequences of human PKA C $\alpha$ /C $\beta$  were obtained from the UniProt [39] and NCBI [40] database resources and from the Ensembl project [41] as described in Materials and Methods S1. Standard BLAST sequence searching algorithms were employed [42] and only sequences with sequence identity (protein level) compared with human PKA C $\alpha$  or C $\beta$  above 75% were included in the dataset for further analysis. The final dataset comprised 41 sequences from placental mammals, including 18 from primates, 5 marsupial sequences, 35 sequences from non-mammalian vertebrates, and 15 from invertebrates (See Materials and Methods S1 and Table S1). Both nucleotide and protein sequences, one single splice variant for each gene, were stored in FASTA format for the total 96 sequences. 81 sequences appear to be full-length, comprising exons 2 to 10 and in addition a 5' exon chosen to correspond to human C $\alpha$ 1/C $\beta$ 1 when possible. Of the incomplete sequences, 8 were missing only the 5' exon. In addition, one *Petromyzon marinus* sequence was missing exons 1, 7, 9, and 10, and the two sequences from *Macropus eugenii* were missing exons 1 and 9, and part of the 3' end, respectively. Finally, the four cartilaginous fish sequences only contain fragments of the full-length sequence.

The sequences were aligned with MUSCLE [43] and the MSAs were viewed and edited with Jalview [44] (See Figure S1). All analysis was subsequently based on MSAs corresponding to exons 2–10 of human PKA C $\alpha$ 1/C $\beta$ 1 (*i.e.* residues 16–350, Fig. 1B) unless otherwise stated, and columns of the MSAs containing gaps were deleted. PHYLIP and NEXUS format files were generated from the FASTA files with a dedicated Perl script. The best model for nucleotide evolution was determined with ModelTest 3.7 [45] in combination with PAUP\* (D. L. Swofford, 2003. PAUP\*, Sinauer Associates, Sunderland, MA) as chosen by the Akaike Information Criterion (AIC). The evolutionary model selected was the general time reversal (GTR) model with a discontinuous gamma distribution ( $\Gamma$ ) for modeling rate heterogeneity over sites and a proportion of invariant sites (I), *i.e.* GTR+ $\Gamma$ +I with four rate categories. The best fitting sequence substitution model for the protein data was determined with ProtTest 2.4 [46], and was found to be, according to the AIC, LG+ $\Gamma$ +I [47]. Also the second best model, JTT+ $\Gamma$ +I [48], was tested for phylogenetic tree construction.

### Phylogenetic Analysis

Bayesian inference of phylogeny was carried out with MrBayes 3.1.2 [49,50] with default heating parameters (three heated Markov chain Monte Carlo chains and one cold) and priors. Two simultaneous and independent runs were carried out with sampling every 10 of 500 k generations until average standard deviation of split frequencies were below 0.01. Branch lengths and majority rule consensus tree topologies were calculated after discarding a burn-in of 100 k generations after which stationarity had been reached. For all calculations presented, the final potential scale reduction factor (PSRF) was below 1.004 for all parameters.

Phylogenetic trees were also generated with the Maximum Likelihood (ML) method employing PhyML 3.0 [51] with default parameters. The robustness of each clade was estimated by a nonparametric bootstrap analysis with 1000 replicates. Gamma distribution parameters, the proportion of invariable sites, branch

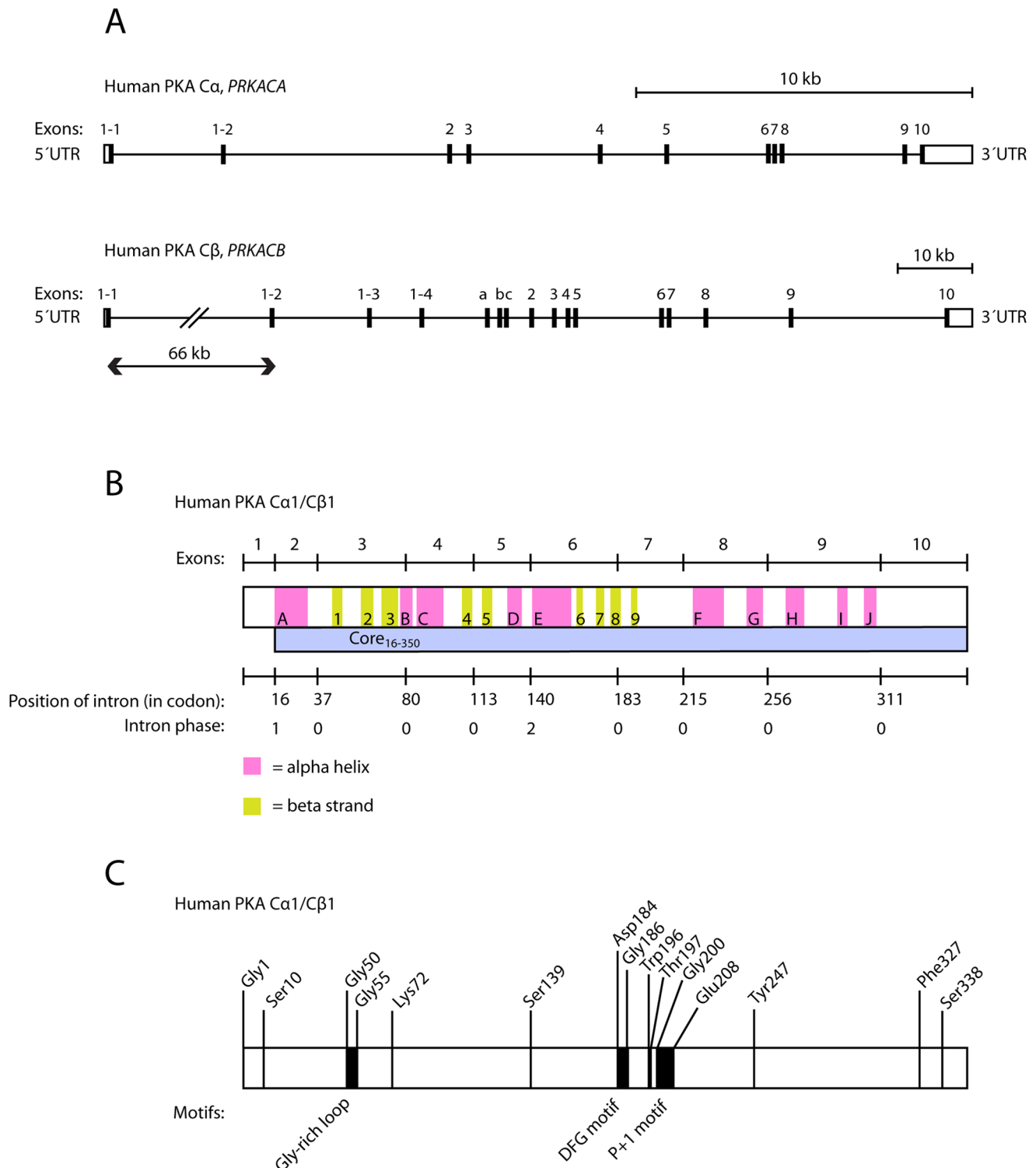


**Figure 1. Gene structure and overview of the human PKA catalytic subunits C $\alpha$  and C $\beta$  encoded by the *PRKACA* and *PRKACB* genes, respectively.** **A** Exons, introns and 3' and 5' untranslated regions (UTRs) of the PKA catalytic subunit genes are shown. The human C $\alpha$  gene (*PRKACA*) is located at chromosome 19p13.1 (reverse strand) and has a length of approximately 26 000 nucleotides (nt). Alternative transcription start sites give rise to two splice variants known as C $\alpha$ 1 and C $\alpha$ 2 (formerly known as C $\alpha$ S). Both splice variants comprise exons 2 to 10 and in addition a 5' exon 1-1 or 1-2 in C $\alpha$ 1 and C $\alpha$ 2, respectively. The human C $\beta$  gene (*PRKACB*) is located at chromosome 1p31.1 (forward strand), with a length of approximately 160 000 nt. Alternative splicing of exons 1-1, 1-2, 1-3 and 1-4 give rise to the splice variants C $\beta$ 1, C $\beta$ 2, C $\beta$ 3 and C $\beta$ 4, respectively. In addition, three short exons, a, b and c, have been shown to be included in the transcript in various combinations. All known enzymatically active isoforms of C $\beta$  comprise exons 2 to 10. **B** Human PKA C $\alpha$ 1 consists of ten  $\alpha$ -helix and nine  $\beta$ -strand secondary structure elements [76]. The figure (middle box) gives the location of  $\alpha$ -helices (pink, A-J) and  $\beta$ -strands (yellow, 1-9) relative to the ten exons and 351 encoded codons of the C $\alpha$ 1 isoform. The locations of the boundaries between exons are given on the upper line. The codons corresponding to the nine introns, as well as their

intron phases, are given on the lower line. The intron phase is defined as the position of the intron within a codon, with phase 0, 1, or 2 lying before the first base, after the first base, or after the second base, respectively. Human PKA C $\beta$ 1 has the same length as C $\alpha$ 1, and the two proteins are differing at only 25 amino acid positions (92.9% sequence identity), strongly suggesting that the overall 3D structures, including secondary structure elements, are close to identical. The position and intron phases for the nine introns are also conserved between human C $\alpha$ 1 and C $\beta$ 1. The sequence segment corresponding to exons 2–10, termed Core<sub>16–350</sub>, is shown as a blue bar. **C** The function of selected important residues and motifs in human PKA catalytic subunits has previously been elucidated in the literature. All listed residues, and their numbering, are identical in C $\alpha$ 1 and C $\beta$ 1, but the research describing these residues and motifs has mainly been performed on C $\alpha$ . Numbering of amino acids is given for mature C $\alpha$ 1 and C $\beta$ 1 (with N-terminal Met removed), both encoding 350 residues. Gly1 is found to be posttranslationally modified by myristoylation [77]. Ser10, Ser139 and Ser338 are well characterized phosphorylation sites [78,79]. The Gly-rich loop (Gly50–Gly55) plays an important role in phosphoryl transfer [80–82]. Lys72 and Asp184 are crucial for ATP and Mg<sup>2+</sup> binding in the active site [81] and the DFG motif (Asp184–Gly186) is conserved in most kinases. The conformation of the motif is critical for the functional state of the kinase [83,84]. Phe327 is the only residue outside of the kinase core binding to the adenine of ATP [82]. Trp196 is an essential residue for R subunit binding and phosphorylation of Thr197 is necessary for the enzyme to assume the active conformation, thereby facilitating catalysis as well as R subunit binding [5,85]. The hydrophobic P+1 motif (Gly200–Glu208) is important for the structure of the enzyme, as well as for substrate recognition [80,86]. Tyr247 competes with cAMP for R subunit binding [5]. doi:10.1371/journal.pone.0060935.g001

lengths and GTR model parameters were all optimized by the ML algorithm from the data. ML phylogenetic trees were also inferred using RAxML 7.2.6 [52], but due to the similarities of the resulting trees only the PhyML results are shown here.

Dendroscope 2.7.4 [53] was used for visualization of phylogenetic trees. Signature sequence logos were generated by applying WebLogo [54]. Calculations were carried out on the University of Oslo Titan computer cluster, mainly through the freely available Bioportal (www.bioportal.uio.no). Protein structure illustrations were generated with PyMOL (W. L. DeLano, The PyMOL Molecular Graphics System, Version 1.3, Schrödinger, LLC). Ratios of nonsynonymous and synonymous substitution rates were calculated with the KaKs\_Calculator [55].

## Results and Discussion

### The PKA C $\alpha$ /C $\beta$ Family is Highly Conserved in Chordates

Vertebrate homologs of human PKA C $\alpha$  and C $\beta$  were extracted from public databases, including Ensembl, UniProt, and database resources provided by the NCBI. New gene models were generated for several of the homologs by careful manual curation (See details in Materials and Methods S1). Homologs, in most cases full-length sequences, were found from 21 placental mammals, the marsupial species opossum (*Monodelphis domestica*) and wallaby (*Macropus eugenii*), chicken, zebra finch (*Taeniopygia guttata*), the Carolina anole lizard (*Anolis carolinensis*), and two and six species of frogs and bony fishes, respectively. In addition, full-length sequences were obtained for the non-vertebrate chordates amphioxus (*Branchiostoma floridae*) and the tunicates *Ciona intestinalis* and *Ciona savignyi*, the echinoderm sea urchin (*Strongylocentrotus purpuratus*), the two mollusks great pond snail (*Lymnaea stagnalis*) and California sea hare (*Aplysia californica*), the hemichordate *Saccoglossus kowalevskii*, the nematode *Caenorhabditis elegans*, the sponge *Amphimedon queenslandica*, as well as six arthropods including honey bee, fruit fly, a tick, and a crustacean. Partial sequences were obtained for orthologs from dogfish shark (*Squalus acanthias*), little skate (*Leucoraja erinacea*) and sea lamprey (*Petromyzon marinus*). In all cases both the nucleotide sequences and the corresponding protein sequences were stored. All sequences are listed in Materials and Methods S1.

We were unable to detect more than a single, reasonably close, PKA C $\alpha$ /C $\beta$  homolog in any of the invertebrate species that were examined. These includes the cephalochordate amphioxus, the urochordates *C. intestinalis*, *C. savignyi* and *Oikopleura dioica*, the echinoderm sea urchin, as well as arthropods, mollusks, a nematode and a sponge. Two homologs were found in most vertebrates, including sea lamprey, and the chondrichthyes *S. acanthias* and *L. erinacea*, while four homologs were detected in a number of bony fishes.

The main isoforms of human *PRKACA* and *PRKACB* comprises exons 2–10 and in addition one or more 5' exons (Fig. 1A). The length of all exons 2–10 and the positions and intron phases of all nine introns are identical in the two human genes (Fig. 1B), clearly demonstrating that these genes arose due to a gene duplication. This structure, reflecting an extreme degree of conservation, is also conserved in all chordate homologs, including the invertebrate cephalochordate amphioxus and the urochordate tunicates and in addition in the echinoderm sea urchin, the hemichordate *S. kowalevskii*, and the crustacean *Daphnia pulex*: the number of exons, their lengths and the codon phases of all introns are identical. The exceptions, apart from the intronless homologs described below, includes the medaka gene encoding a protein with Ensembl identifier ENSORLP00000018527. This gene appears to have acquired a new 88-nucleotide intron (intron phase 0) in the middle of exon 9. In addition, the basal metazoan *A. queenslandica* has an additional intron of 334 nucleotides that splits the coding sequence corresponding to vertebrate exon 6.

The number of codons encoded by exons 2–10 in the *PRKACA/B* family of genes - corresponding to residues 16–350 in human proteins PKA C $\alpha$ 1/C $\beta$ 1 - is consequently also identical in all species listed above. We term this sequence segment Core<sub>16–350</sub> (Fig. 1B) in order to distinguish it from the variable 5' exons. The genomic data for the mollusks are not yet available in the public domain and the intron/exon structure is currently unknown, but in insects the protein coding segment of the *PRKACA/B* homologs are contained in a single exon. Nevertheless, the insect homologs also have the same number of residues for the segment corresponding to Core<sub>16–350</sub>. An MSA of all sequences with full-length Core<sub>16–350</sub> is shown in Figure S1. Consequently, we find that nearly all our PKA C $\alpha$ /C $\beta$  homologs from Bilateria have the same length for the Core<sub>16–350</sub>, and with variable length N-termini corresponding to the multitude of isoforms. The only exceptions are a single-residue insertion after human PKA C $\alpha$ 1 Lys63, in the middle of exon 3, in both homologs from mollusks and a single-residue insertion after human PKA C $\alpha$ 1 Ala38 in a fast-evolving sequence from opossum (identifier ENSMODP00000015141). These insertions are in loop structures in PKA C $\alpha$ 1 (See e.g. [56] for the 3D structure) and are expected to be compatible with an unchanged overall 3D structure of the kinase.

Pairwise sequence identity between any of the bilaterian PKA C $\alpha$ /C $\beta$  homologs described above is always above 77% for the 335 residues of the Core<sub>16–350</sub> at the amino acid level. Leaving out the fast-evolving sequences from marsupials and a single fast-evolving zebrafish sequence (Q7T374), the sequence identities are always above 80% and 87% within the chordates and vertebrates, respectively. This demonstrates very strong purifying selection and an exceptionally high degree of sequence conservation for this protein family.

## The PKA C $\alpha$ /C $\beta$ Gene Family Contains Several Putative Retroposons

In addition to the *PRKACA/B* homologs that have conserved exon/intron structure in chordates and several other deuterostomes, and the arthropod homologs, also with several exons, but with the protein coding segment contained in a single exon, a number of intronless *PRKACA/B* homologs are found in vertebrate genomes. Among these are human *PRKACG*, located on chromosome 9 between the genes *PIP5K1B* and *FXN*, but transcribed in the opposite direction. Intronless *PRKACG* has the same number of codons as the PKA C $\alpha$ 1-like transcript of *PRKACA* and is conserved in the great apes, in chimpanzee, gorilla, and orangutan and in the Old World monkeys rhesus macaque and hamadryas baboon (Sequences are listed in Materials and Methods S1). Genome browsing at the Ensembl resource also shows the synteny to be conserved in these species with *PIP5K1B* and *FXN* being transcribed in one direction and *PRKACG*, located between these two genes, in the opposite. Between *PIP5K1B* and *FXN* in the gibbon (*Nomascus leucogenys*) genome, a species more closely related to great apes than the Old World monkeys, there is no full-length *PRKACG* ortholog, but instead a putative *PRKACA/B* pseudogene with several frame shifting mutations. We find no evidence of *PRKACG* orthologs in prosimian primates such as greater galago (*Otolemur garnettii*), tarsier (*Tarsius syrichta*), or gray mouse lemur (*Microcebus murinus*), although the last two of these have genomes that are still fragmented and with undisclosed synteny around the genes *PIP5K1B* and *FXN*. In the common marmoset (*Callithrix jacchus*) genome, there is a fragment, most likely not protein-coding, of *PRKACG* between *PIP5K1B* and *FXN*, corresponding to PKA C $\alpha$ 1 residues 21–350. Finally, in the mouse and dog genomes, *PIP5K1B* and *FXN* are neighboring genes being transcribed in the same direction, but without any sign of a *PRKACA/B* homolog in this region.

These findings strongly support the previous suggestion that *PRKACG* is a retroposon due to a PKA C $\alpha$ 1-type transcript [35] that has been inserted between *PIP5K1B* and *FXN* in a common ancestor of great apes and Old and New World monkeys. The putative *PRKACG* transcripts could potentially give rise to functional kinases in all great apes and in the Old World monkeys, but not in gibbons and the New World monkey marmoset where there are mutations disrupting the reading frame in the *PRKACG* retroposon. In the marmoset genome, there is in addition to the putative *PRKACG* pseudogene on chromosome 1, a second retroposon (Ensembl identifier ENSCJAP00000040924) related to PKA C $\alpha$ 1 on chromosome 2. This gene was not found in other primates.

In addition to the PKA C $\alpha$ 1-like retroposons in primates, we found intronless *PRKACA* homologs in the two sequenced genomes of marsupials, the wallaby kangaroo (*M. eugenii*) and the Brazilian opossum (*M. domestica*) (See Materials and Methods S1). Also these putative retroposons appear to be derived from a PKA C $\alpha$ 1-type transcript, but are otherwise unrelated to primate *PRKACG*.

## Elucidating the Phylogeny of the PKA C $\alpha$ /C $\beta$ Family is Nontrivial Due to High Sequence Conservation

The distribution of PKA C $\alpha$ /C $\beta$  homologs in Bilateria, as well as phylogenetic trees generated with unsophisticated hierarchical clustering methods (results not shown), suggest that this gene family has expanded through repeated gene duplication events in vertebrates. However, despite numerous attempts, state-of-the-art probabilistic methods, both Bayesian inference and maximum likelihood (ML) methods, were not able to generate a statistically strongly supported phylogenetic tree for the full PKA C $\alpha$ /C $\beta$

family from the complete data set. After careful analysis of the data (*vide infra*), we were nevertheless able to derive reliable phylogenies for this gene family by dividing the data into subsets. The final phylogenetic trees were generated as follows: an MSA was generated from the nucleotide sequences corresponding to the Core<sub>16–350</sub> segment for selected vertebrates, amphioxus, sea urchin and fruit fly. After removal of all nucleotides at codon position 3, the dataset was employed to generate Bayesian inference and ML trees, with identical topology, for the PKA C $\alpha$ /C $\beta$  homologs with good Bayesian posterior probabilities and bootstrap support for the major nodes. The phylogram was rooted with the sea urchin and fruit fly as outgroups (Fig. 2). Bayesian inference methods were also used to generate a phylogenetic tree of 22 vertebrate PKA C $\alpha$  orthologs employing human and mouse PKA C $\beta$  as outgroups (Fig. 3A). Similarly, a tree with 26 PKA C $\beta$  orthologs was generated with human and mouse PKA C $\alpha$  as outgroups (Fig. 3B). These trees, and trees from the corresponding ML analysis, are based on MSAs for the nucleotide sequences with all three codon positions included.

Neither Bayesian inference nor ML methods, generally accepted to be the most accurate [57,58], were able to generate a reliable phylogeny for the PKA C $\alpha$ /C $\beta$  family from the full data set. This was not due to unreliable MSAs as only three of the sequences in the original data set each had single codon insertions (*vide supra*) and manual removal of these was trivial. The problem, however, appears to be a combination of weak phylogenetic signals and problematic nonphylogenetic signals in the data. Due to the very high level of sequence conservation, the protein data set contains few phylogenetically informative sites, *i.e.* amino acid sites that favor one phylogenetic tree topology over others. As an example, for the 22 chordate taxa used to generate the tree in Fig. 2, the corresponding amino acid data set has 335 columns/sites. Of these, only 58 sites are phylogenetically informative, while 255 are fully conserved and identical for all taxa and the remaining 22 are autapomorphic. Unsurprisingly, protein data phylogenetic trees generated with two recommended substitution models (LG/JTT+ $\Gamma$ +I) and well-tested ML programs (PhyML/RAXML) were overall fairly similar, but with very poor bootstrap support. The trees generated with various subsets of the available taxa were incongruent and also in several cases inconsistent with the known evolutionary relationship between the various chordate species.

In order to secure a stronger phylogenetic signal [59], the nucleotide data set was employed for deriving the phylogenetic relations. For the 22 chordate taxa in Fig. 2, there are 77, 33, and 312 phylogenetically informative sites (out of 335 sites in total) for codon position 1, 2, and 3, respectively. The low number of informative sites at codon position 1 and 2 reflects the high degree of conservation at the amino acid level, while the high number at codon position 3 (93%) reflects the large time-span since the common ancestor of these genes. For all tested nucleotide data sets, the GTR+ $\Gamma$ +I model was predicted to be superior. While using the nucleotide sequences for deriving the phylogenetic relationships ensures a stronger phylogenetic signal, in particular the data from codon position 3, due to the degeneracy of the genetic code, may be severely mutationally saturated due to reversions and convergences that erase the true phylogenetic signal. This will especially be problematic for inferring ancient phylogenies [59], where long branch attraction (LBA), *i.e.* a tendency for grouping of lineages with long branches irrespective of their true relationships, may lead to misleading phylogenies [60]. In particular, fast-evolving genes may artificially occur too deeply in the tree due to LBA towards the outgroups.

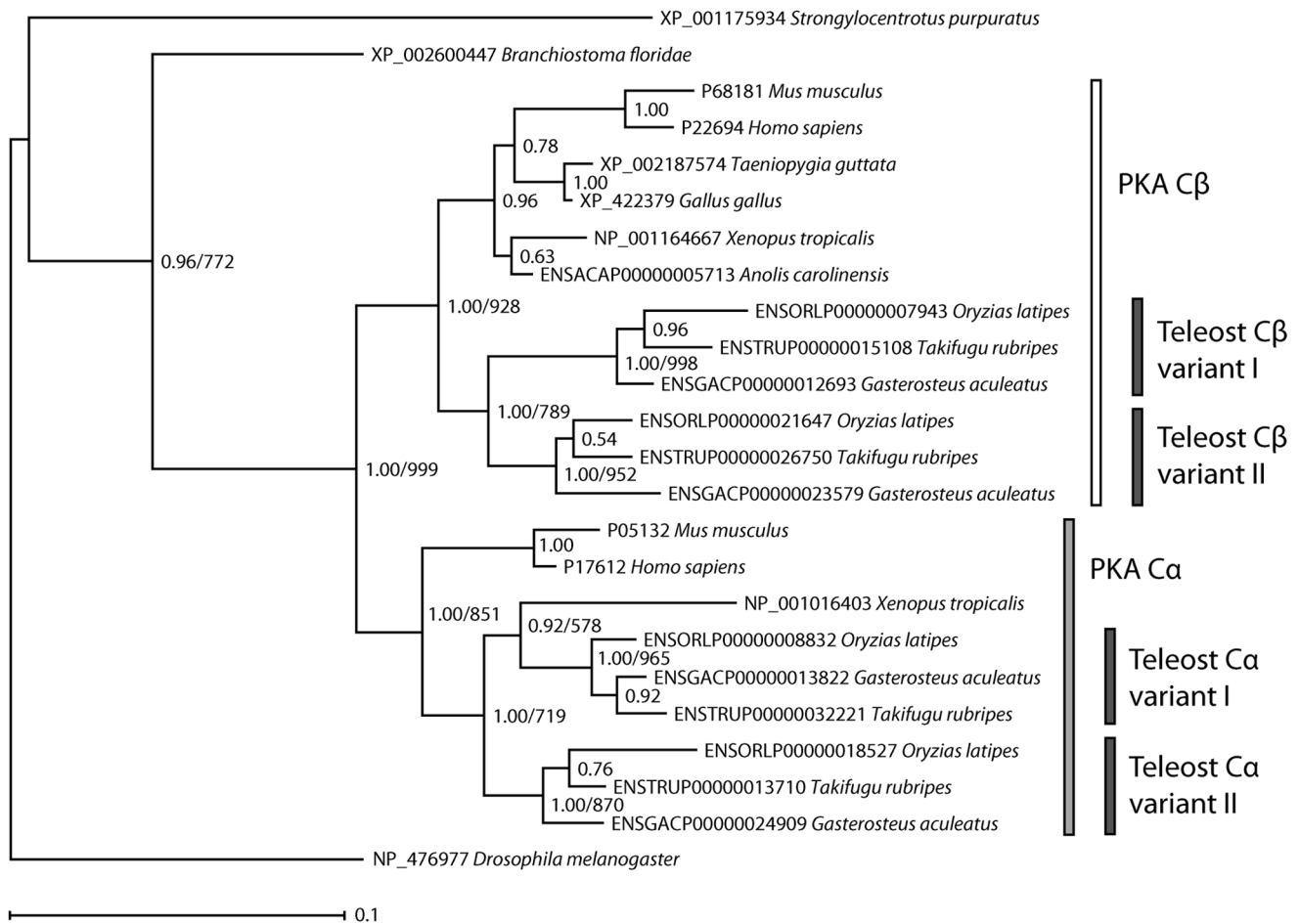


**Figure 2. Phylogenetic relationships among the PKA catalytic subunit homologs in chordates.** The  $C\alpha$  and  $C\beta$  paralogs are a result of a gene duplication in a common ancestor of vertebrates. Subsequent duplications of  $C\alpha$  and  $C\beta$  in a teleost fish ancestor have resulted in four PKA catalytic subunits in these organisms. The Bayesian inference tree is based on the nucleotide sequences (codon positions 1 and 2 only, GTR+ $\Gamma$ +I model) of exons 2 to 10 which corresponds to a multiple sequence alignment with no gaps. The phylogram is shown with estimated branch lengths proportional to the number of substitutions at each site, as indicated by the scale bar. The arthropod fruit fly (*D. melanogaster*) and the echinoderm sea urchin (*S. purpuratus*) have been set as outgroups. Bayesian posterior probabilities are shown for each node. The topology of a maximum likelihood (ML) tree generated with the same data set and model was identical to the Bayesian inference tree. ML bootstrap values are shown for selected nodes (1000 replications). The sequences of human and mouse PKA  $C\alpha$  and  $C\beta$  and the homologs from amphioxus (*B. floridae*), zebra finch (*T. guttata*), chicken (*G. gallus*), the frog *X. tropicalis*, the lizard *A. carolinensis*, medaka (*O. latipes*), the pufferfish *T. rubripes*, and stickleback (*G. aculeatus*) are described in Materials and Methods S1. The *X. tropicalis*  $C\alpha$  and *A. carolinensis*  $C\beta$  are incorrectly placed (See discussion and Fig. 3). doi:10.1371/journal.pone.0060935.g002

As for the protein data set, trees generated with subsets of the available taxa were highly incongruent and in several cases with pronounced LBA, clearly demonstrating a strong nonphylogenetic signal. In order to secure minimal nonphylogenetic signals and reduce LBA, codon position 3 sites were removed from the data set used to generate the phylogeny in Fig. 2. In addition, fast-evolving taxa such as the tunicate [61], marsupial PKA  $C\alpha/C\beta$  homologs and the primate PKA  $C\gamma$  homologs were left out of the data set. Fig. 2 is expected to describe the ancient evolution of the PKA  $C\alpha/C\beta$  family in chordates correctly, with the gene duplications in the common ancestor of vertebrates as well as in teleost fishes supported by high Bayesian posterior probabilities and strong bootstrap support for the ML analysis.

In order to better describe the evolution of the two PKA  $C\alpha$  and PKA  $C\beta$  paralogs in vertebrates separately, the trees in Fig. 3 were generated. Reliable phylogenies could not be generated from a data set containing codon positions 1 and 2 only, as in Fig. 2, most likely due to weak phylogenetic signals in the data. However,

for the relatively recent phylogenetic relations in Fig. 3, the saturation at codon position 3 is expected to be less severe and all three codon positions were included in the data set for analysis. In Fig. 2, there are two errors due to nonphylogenetic signal. These are the placement of frog PKA  $C\alpha$  in a clade together with teleost fish and the erroneous lizard/frog PKA  $C\beta$  clade. Both these errors are corrected in Fig. 3 upon inclusion of codon position 3 data. The most ancient splittings, however, are unreliable in Fig. 3, in particular the description of the branching between the tetrapod and teleost fish PKA  $C\alpha$  homologs as a multifurcation (Bayesian analysis) or two bipartitions with extremely poor bootstrap support (ML analysis, not shown) in Fig. 3A.

In conclusion, while the phylogenies of the PKA  $C\alpha$  and PKA  $C\beta$  subfamilies, especially within the tetrapods, appears to be correctly inferred from the full nucleotide dataset (Fig. 3), the ancient evolution of the PKA  $C\alpha/C\beta$  family in chordates is correctly described with cladistic methods only after removal of codon position 3 data (Fig. 2). The protein data set contains

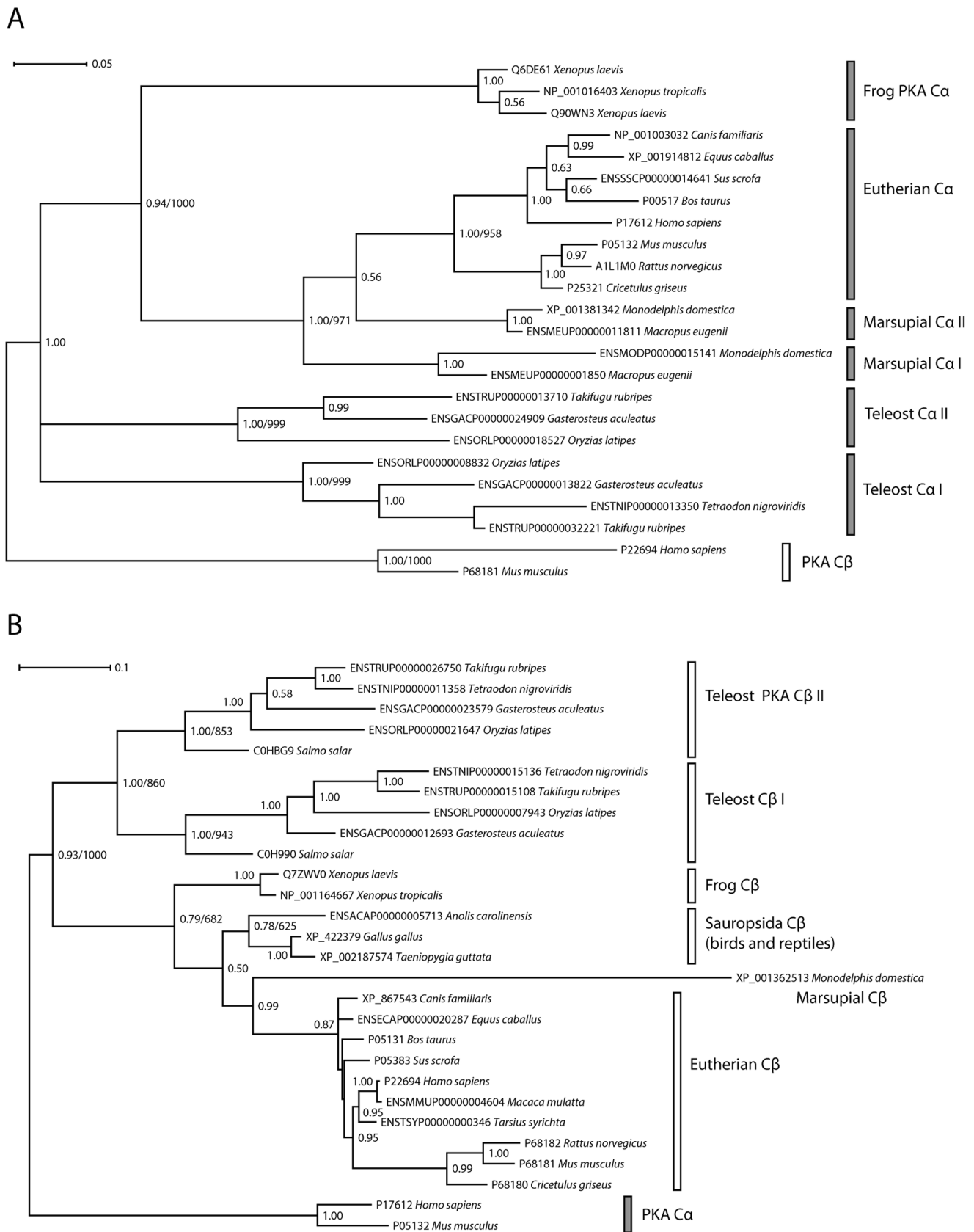


**Figure 3. The Bayesian inference trees for vertebrate PKA  $\alpha$  and  $\beta$  both closely reflects the evolutionary relationships among these organisms. A** Phylogenetic analysis of  $C\alpha$  orthologs resulted in a tree that was rooted with human and mouse  $C\beta$  as outgroups. The tree was based on the nucleotide sequences of exons 2 to 8 (all codon positions, GTR+ $\Gamma$ +I model). **B** Phylogenetic analysis of  $C\beta$  orthologs was performed

employing nucleotide sequence data (all codon positions, exons 2 to 10, GTR+ $\Gamma$ +I model). The resulting tree was rooted with human and mouse C $\alpha$  as outgroups. In both trees, branch lengths are shown as substitutions per site, with scale indicated by the scale bars. Bayesian posterior probabilities are given for each node and ML bootstrap values (1000 replications) are shown for selected nodes where the clades are identical in the Bayesian and ML analysis. In addition to organisms found in Fig. 2, representative sequences from the following species were included: eutherian mammals rhesus macaque (*M. mulatta*), tarsier (*T. syrichta*), dog (*C. familiaris*), horse (*E. caballus*), pig (*S. scrofa*), cow (*B. taurus*), rat (*R. norvegicus*), and hamster (*C. griseus*), marsupial mammals wallaby (*M. eugenii*) and opossum (*M. domestica*), the frog *X. laevis*, the pufferfish *T. nigroviridis* and Atlantic salmon (*S. salar*). See Materials and Methods S1 for the sequence data. doi:10.1371/journal.pone.0060935.g003

limited phylogenetic information and does not give reliable phylogenies in chordates. No analysis based on partitioned data, for example according to codon position, was attempted, as this is likely to lead to overparametrization.

### Phylogenetic Inferences for the PKA C $\alpha$ /C $\beta$ Family in the Chordate Lineage

The well-resolved phylogenetic tree in Fig. 2 strongly suggests the following sequence of events during the evolution of the PKA C $\alpha$ /C $\beta$  gene family: a single PKA C $\alpha$ /C $\beta$ -like gene in the common ancestor of chordates, arthropods and echinoderms was duplicated in a common ancestor of vertebrates, which lead to the two paralogous genes corresponding to PKA C $\alpha$  and C $\beta$ . These two genes were again duplicated in a common ancestor of teleost fishes, leading to paralogs that we suggest are denoted PKA C $\alpha$ -I, C $\alpha$ -II, C $\beta$ -I, and C $\beta$ -II.

The data indicates that the first PKA C $\alpha$ /C $\beta$  gene duplication, resulting in PKA C $\alpha$  and PKA C $\beta$ , took place after the divergence of the urochordate and cephalochordate lineages. Currently there are only fragments of PKA C $\alpha$ /C $\beta$  homologs available in public databases for the chondrichthyes (dogfish shark and little skate) and the cyclostome sea lamprey (Table S1), but the PKA C $\alpha$ /C $\beta$  homologs also in these organisms appear to occur in pairs. Unfortunately, the phylogenetic signal in the data is too weak to classify these sequences as PKA C $\alpha$  or PKA C $\beta$ , and to exclude the possibility that these paralogous gene pairs are results of independent gene duplications, but the most parsimonious explanation for this distribution of PKA C $\alpha$ /C $\beta$  homologs is that a single PKA C $\alpha$ /C $\beta$  gene duplication occurred before the divergence of the jawless fish lineage and the subsequent divergence of sharks and skates. Interestingly, this timing of the PKA C $\alpha$ /C $\beta$  gene duplication coincides with the two rounds (2R) of whole genome duplication (2R hypothesis) that took place after the emergence of the invertebrate chordates and before the radiation of jawed vertebrates [62–64]. The PKA C $\alpha$  and PKA C $\beta$  gene split is thus likely to have occurred in the Cambrian, roughly 500 Mya [65,66]. Canaves and Taylor [38] found that the gene duplications of the PKA regulatory subunits resulting in the paralogs RI $\alpha$  and RI $\beta$  as well as RII $\alpha$  and RII $\beta$  also occurred in the chordate lineage, suggesting that the gene duplications of the R and C subunits might have taken place simultaneously.

The secondary duplications of PKA C $\alpha$  and PKA C $\beta$  (Figs. 2 and 3) appear to be unique to teleost fishes, and might have coincided with the teleost whole genome duplication that took place 226–316 Mya [67,68]. Finally, the presence of two *X. laevis* PKA C $\alpha$  paralogs and a single *X. tropicalis* PKA C $\alpha$  (Fig. 3A) in the amphibian genomes is consistent with the recent whole genome duplication event in the common ancestor of the *X. laevis* group not found in *X. tropicalis* [69,70].

As expected, both the subtrees for PKA C $\alpha$  (Fig. 3A) and PKA C $\beta$  (Fig. 3B) have eutherian clades with the marsupial orthologs as sister clades, and with Sauropsida (birds and reptiles, Fig. 3B only) and frogs appearing as sister clades deeper into the phylogenetic tree. We were unable to find the PKA C $\alpha$  gene in any of the released genomes of Sauropsida, and this clade is consequently

missing in Fig. 3A. However, a single EST (expressed sequence tag) sequence from a chicken testis library (GenBank identifier CN229123 [71]) appears to confirm the presence of PKA C $\alpha$  also in birds. Several vertebrate species are missing either PKA C $\alpha$  or PKA C $\beta$  in the current genomic data sets, but this is most likely due to low sequence coverage in unfinished genomes. We find no evidence for extensive PKA C $\alpha$  or C $\beta$  gene loss in any of the main vertebrate groups.

The marsupial *M. domestica* PKA C $\beta$  appears to be particularly fast-evolving (Fig. 3B). The *M. eugenii* PKA C $\beta$  ortholog is present in the genome, but the full sequence is currently unknown. Both marsupial genomes [72,73] have two PKA C $\alpha$  paralogs. Marsupial PKA C $\alpha$ -I has the same exon/intron structure as PKA C $\alpha$  in all other mammals. Marsupial PKA C $\alpha$ -II, however, is intronless and a putative PKA C $\alpha$  retroposon (Fig. 3A). The full-length sequences are not at present available for all the marsupial PKA C $\alpha$  homologs, but interestingly, intronless PKA C $\alpha$ -II appears to be significantly more conserved than the ancestral variant PKA C $\alpha$ -I. The 5' segment of the two marsupial PKA C $\alpha$ -II orthologs (only the 232 5' codons are available in the sequence for *M. eugenii*) have 17 synonymous and no non-synonymous mutations, suggesting strong purifying selection. For PKA C $\alpha$ -I, the 294 codons corresponding to exons 2–9 (exons 1 and 10 are missing in the current *M. eugenii* genomic sequence) have 70 mutations, including a 3 nucleotide insertion in opossum PKA C $\alpha$ -I, and 21 of these are non-synonymous. These data, although limited, strongly suggests that the retroposon PKA C $\alpha$ -II have become functional in marsupials and that the purifying selection acting upon PKA C $\alpha$ -I and PKA C $\beta$  has become less stringent.

### Vertebrate PKA C $\alpha$ and C $\beta$ Mainly Differs in the C-tail and in Subdomains I and II

In order to elucidate the potential differences between the PKA C $\alpha$  and PKA C $\beta$  protein subfamilies, an MSA of all available vertebrate homologs was generated. In this set of 27 PKA C $\alpha$  and 33 PKA C $\beta$ , there are within the 335 sites/columns of the Core<sub>16–350</sub> only 62 sites (19%), that are phylogenetically informative while 235 sites are fully conserved in all taxa, again reflecting the very high degree of purifying selection. A manual inspection of the MSA showed that eleven sites/columns could tentatively be used to discriminate between the two PKA subfamilies. Sequence logos for these eleven sites are shown in Fig. 4. Human PKA C $\alpha$ 1 residues Gln35, Thr37, Glu64, Gly66, His68, Ser109, and Glu334 are fully conserved in all vertebrate PKA C $\alpha$ , while at the corresponding sites in PKA C $\beta$  the sequence conservation is less stringent. Similarly, human PKA C $\beta$ 1 residues Asp42, Gln67, Arg319 are fully conserved in vertebrate PKA C $\beta$  (Fig. 4). The single site where there is no overlap between amino acid use in the two subfamilies is at residues 66 where PKA C $\alpha$  and C $\beta$  have Gly and Glu/Asn/Asp, respectively.

The residues that correspond to the eleven sites that tentatively discriminates between the subfamilies PKA C $\alpha$  and C $\beta$  are all exposed at the protein surface, in or close to loop structures, in subdomains I and II and in the C-tail (Fig. 5). None of these residues are located close to the kinase active site and their identity



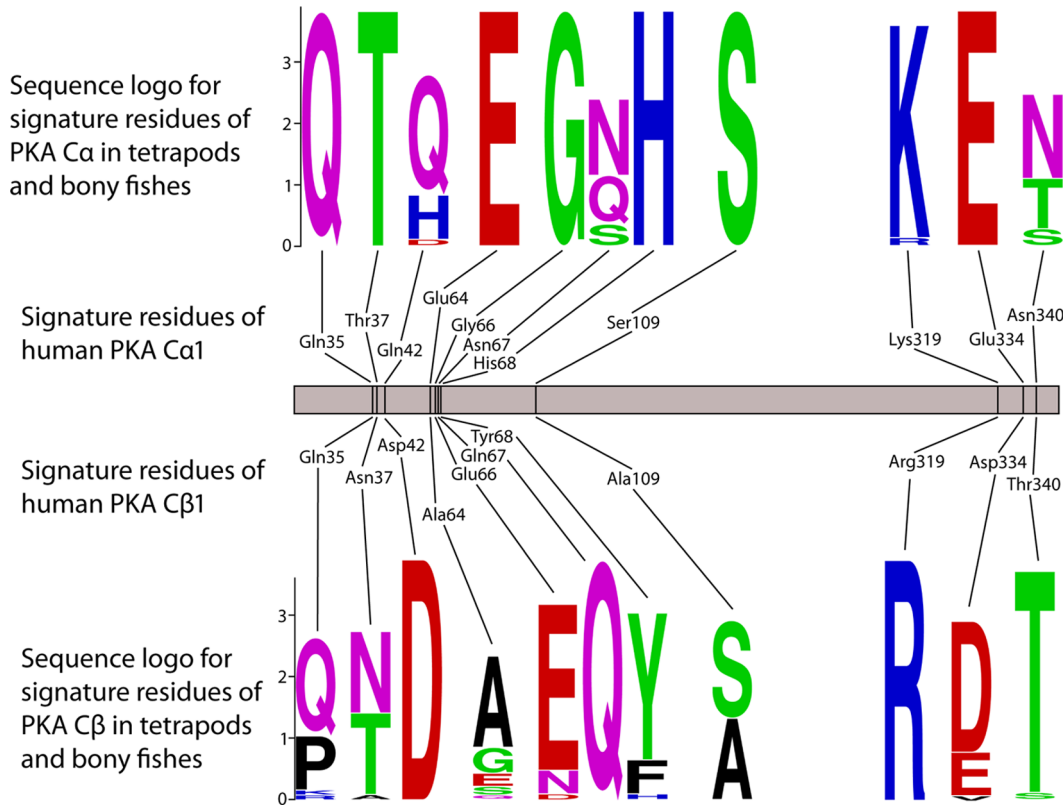


**Figure 4. The identity of eleven amino acids in the protein chain may define the C $\alpha$  and C $\beta$  branches of PKA catalytic subunits.** Our full set of PKA catalytic subunits (Materials and Methods S1) from bony fishes and tetrapods, comprising 27 C $\alpha$  and 33 C $\beta$ , was employed to identify eleven amino acid positions that together may be used to classify a PKA catalytic subunit as belonging to one of the two branches. The sequence logos define the PKA C $\alpha$  and C $\beta$  clades within the *Teleostomi*, which includes the familiar classes of bony fishes, birds, mammals, reptiles, and amphibians. We find invariable Gln35, Thr37, Glu64, Gly66, His68, Ser109 and Glu334 in C $\alpha$  and invariable Asp42, Glu67, and Arg319 in C $\beta$  (C $\alpha$ 1/C $\beta$ 1 numbering). The residues in the corresponding positions in human C $\alpha$ 1 and C $\beta$ 1 are also shown. doi:10.1371/journal.pone.0060935.g004

is not likely to affect PKA kinase activity. Likewise, they are not located near the protein surface segments that are known to interact with the PKA regulatory subunits (Fig. 5B), and these residues should not be important for R subunit interactions. Several of the eleven residues, especially residues 64, 319, 334 and 340, are protruding their side chains into the solvent and might be targets for PKA C $\alpha$ - or PKA C $\beta$ -specific post-translational modifications and/or protein-protein interactions. Particularly, Glu64 is conserved in all vertebrate PKA C $\alpha$ , while residue 64 is variable in 33 C $\beta$ , being Ala in all mammals and Glu in only three fish homologs. In PKA C $\beta$  Glu66 is absolutely conserved, except in five of the fish homologs, while this residue is conserved as Gly in C $\alpha$ .

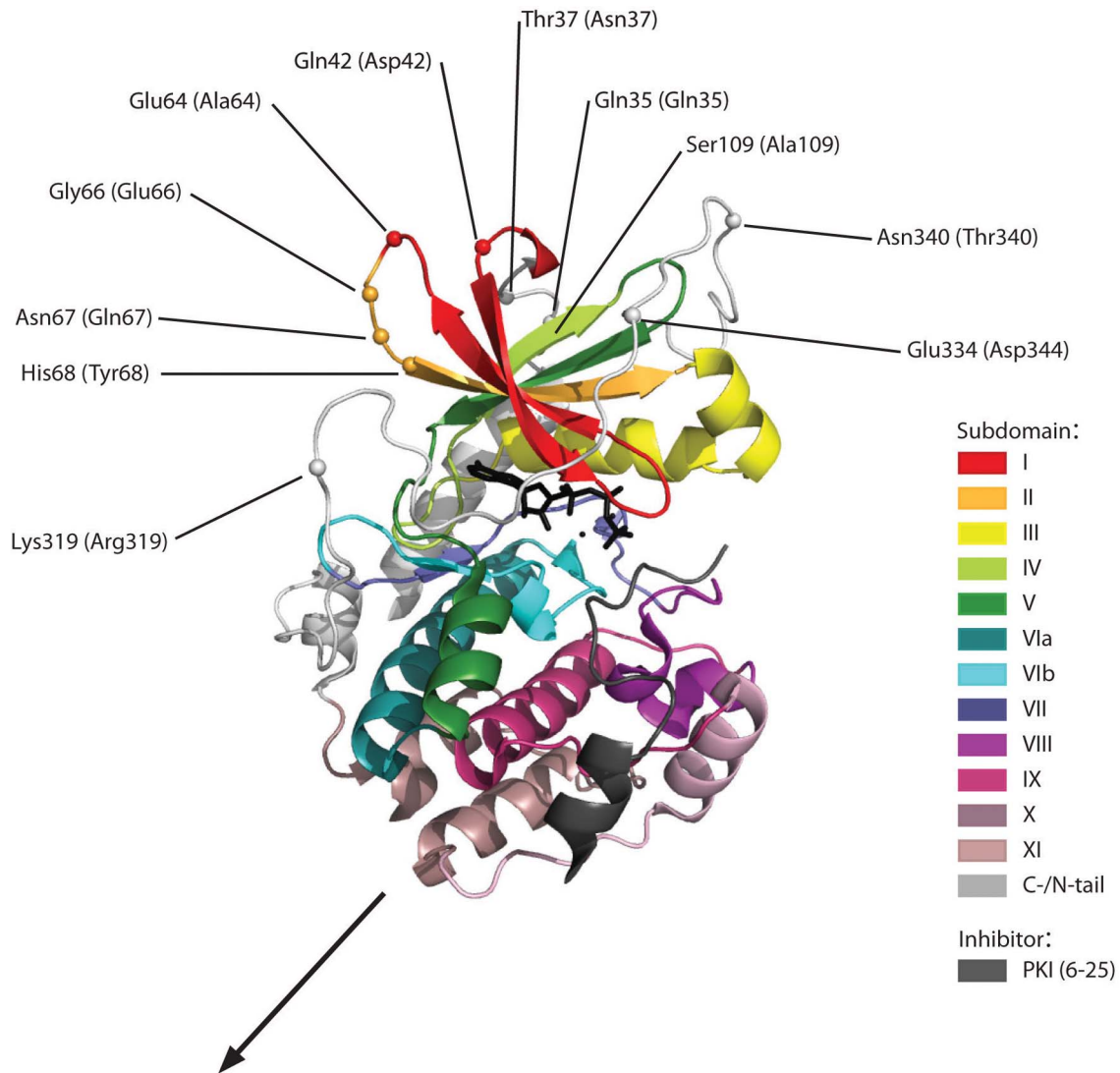
#### Strong Purifying Selection is Lost in PKA C $\gamma$

A comparison of PKA C $\alpha$ 1 from human and the galago, a prosimian primate, shows that there are 59 and 4 synonymous (silent) and non-synonymous (amino acid changing) mutations, respectively. Between human and macaque PKA C $\gamma$  there are slightly fewer, 44, mutations, but from these 31 amino acid changes, indicating that the strong purifying selection in the PKA C $\alpha$  lineage is lost in PKA C $\gamma$ . A powerful tool for evaluating the evolution of protein coding sequences, is calculating the ratio of the non-synonymous ( $K_a$ ) and synonymous ( $K_s$ ) substitution rates, where  $K_s$  is the number of synonymous substitutions per synonymous site and  $K_a$  is the number of non-synonymous

substitutions per non-synonymous site [74]. A  $K_a/K_s < 1$  indicates purifying (negative) selection,  $K_a/K_s > 1$  is a sign of positive selection, while  $K_a/K_s \sim 1$  indicates neutral evolution of the protein. Table 1 shows  $K_a/K_s$  for comparisons of five representative tetrapod PKA C $\alpha$  homologs and five primate PKA C $\gamma$  homologs. Due to missing sequences in the databases it was not possible to compare the same species for C $\alpha$  and C $\gamma$ . For the PKA C $\alpha$  sequences, the average  $K_a/K_s$  is 0.011. PKA C $\alpha$  sequences were also compared for other placental mammals and  $K_a/K_s$  were found to be in the range 0.004–0.023.  $K_a/K_s$  for a comparison of human PKA C $\alpha$  and C $\beta$ , and of the human and mouse PKA C $\beta$  orthologs, were 0.0076 and 0.0198, respectively. These data for the PKA C $\alpha$ /C $\beta$  homologs in placental mammals again confirms the very strong purifying selection acting upon these kinases.

The  $K_a/K_s$  values from the comparison of the primate PKA C $\gamma$  sequences in Table 1 are in the range 0.14–1.36. Due to the fairly close evolutionary relationships between these species, the number of mutations in *PRKACG* transcripts between these species is rather low, for example 9, 31 and 46 between human and chimpanzee, orangutan, and macaque, respectively. Consequently, the  $K_a/K_s$  values are not expected to be highly reliable, but the average value of 0.45 clearly suggests that the strong purifying selection in the PKA C $\alpha$  lineage is lost in PKA C $\gamma$ . This finding that mutations in PKA C $\gamma$  appear to be neutral, combined with the loss of a functional C $\gamma$  in gibbons and marmoset (*vide supra*), suggest that there are no evolutionary constraints on maintaining a functional PKA C $\gamma$  protein in higher primates. However, this analysis does

A



B

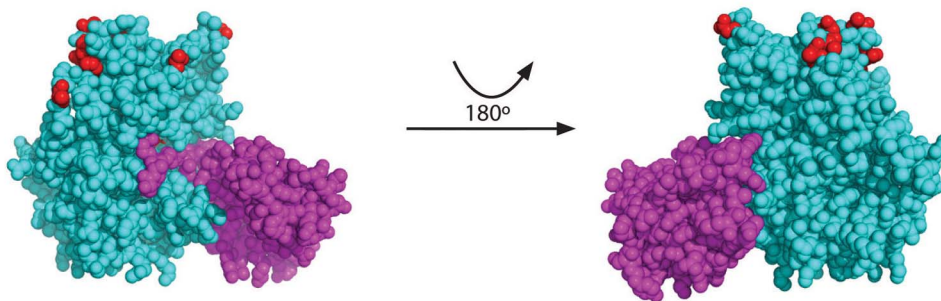


**Figure 5. Signature residues defining PKA C $\alpha$  and C $\beta$  do not interact with ATP, peptide inhibitor PKI $\alpha$  or the kinase regulatory subunit.** **A** The tentative signature residues of PKA C $\alpha$  and C $\beta$  (Fig. 4) are highlighted in a structural model of PKA C $\alpha$ 1 in complex with a truncated PKI $\alpha$  (residues 6–25). Signature amino acids in human C $\alpha$ 1 and C $\beta$ 1 are shown without and within parenthesis, respectively. The conserved kinase core has been divided into subdomains (represented in different colors) [87] as defined by Hanks and Hunter [88]. ATP is rendered as sticks (black) and two divalent cations as black spheres. The model is based on the experimental structure of Thompson *et al.* [56] (PDB identifier 3FJQ). **B** Residues in C $\alpha$ 1 (cyan) interacting with regulatory subunit RI $\alpha$  (purple, residues 92–245 of bovine RI $\alpha$  only) are mainly restricted to the large lobe and do not overlap with any of the C $\alpha$  signature residues (red). The complex is shown with the same orientation of C $\alpha$ 1 as in panel A (left) and rotated 180° (right). The model is based on the experimental structure of Kim *et al.* [5] (PDB identifier 3FHI). doi:10.1371/journal.pone.0060935.g005

**Table 1.** Ratio of amino acid replacing (*Ka*) and silent (*Ks*) mutation rates for all pairwise comparisons of five tetrapod PKA C $\alpha$  homologs and five primate PKA C $\gamma$  homologs.

	<i>Ka/Ks</i> <sup>a</sup>			
	<i>H. sapiens</i> C $\alpha$	<i>O. garnettii</i> C $\alpha$	<i>M. musculus</i> C $\alpha$	<i>B. taurus</i> C $\alpha$
<i>O. garnettii</i> C $\alpha$	0.0159 (0.0158)			
<i>M. musculus</i> C $\alpha$	0.0141 (0.0141)	0.0230 (0.0226)		
<i>B. taurus</i> C $\alpha$	0.0064 (0.0063)	0.0116 (0.0111)	0.0156 (0.0158)	
<i>X. tropicalis</i> C $\alpha$	0.0065 (0.0060)	0.0055 (0.0056)	0.0065 (0.0064)	0.0059 (0.0060)
	<i>Ka/Ks</i> <sup>b</sup>			
	<i>H. sapiens</i> C $\gamma$	<i>P. troglodytes</i> C $\gamma$	<i>P. pygmaeus</i> C $\gamma$	<i>G. gorilla</i> C $\gamma$
<i>P. troglodytes</i> C $\gamma$	0.135 (0.127)			
<i>P. pygmaeus</i> C $\gamma$	0.290 (0.324)	0.175 (0.194)		
<i>G. gorilla</i> C $\gamma$	1.360 (1.207)	0.162 (0.148)	0.295 (0.319)	
<i>M. mulatta</i> C $\gamma$	0.697 (0.678)	0.419 (0.406)	0.393 (0.393)	0.621 (0.603)

<sup>a</sup>*Ka/Ks* ratios for pairwise comparisons of PKA C $\alpha$  from human, a prosimian primate (*O. garnettii*), mouse (*M. musculus*), cattle (*B. taurus*) and a frog (*X. tropicalis*) calculated according to the model of Goldman and Yang [89] and the model averaging method of Zhang *et al.* (in parenthesis) [90] for the Core<sub>16–350</sub> sequence segment.

<sup>b</sup>*Ka/Ks* ratios for pairwise comparisons of PKA C $\gamma$  from human, chimpanzee (*P. troglodytes*), orangutan (*P. pygmaeus*), gorilla (*G. gorilla*) and rhesus macaque (*M. mulatta*) calculated as described above.

doi:10.1371/journal.pone.0060935.t001

not exclude the possibility that the PKA C $\gamma$  transcript has an important function in humans, great apes and other Simiiformes, for example in regulation of PKA C $\alpha$ /C $\beta$  transcript processing [75].

## Conclusion

We have shown that the PKA C $\alpha$  and C $\beta$  catalytic subunits found in chordates and other animal species builds a phylogenetic clade of kinases with a very high degree of conservation at the protein level. In the core segment corresponding to exons 2–10 of vertebrate C $\alpha$ 1/C $\beta$ 1 the synonymous mutation rate is approximately two orders of magnitude larger than the amino acid changing mutation rate. All the main residues and sequence segments previously shown to be important for human C $\alpha$ /C $\beta$  function (Fig. 1C), including the phosphorylation sites, the ATP and Mg<sup>2+</sup> interacting residues and the DFG and P+1 motifs, are basically fully conserved in all homologs in chordates, insects and other animal sequences investigated in the current study. The few residues that differ in C $\alpha$  and C $\beta$  (Fig. 4) should be investigated in order to elucidate possible functional differences between the two paralogs. Finally, the C $\alpha$ 1-derived expressed retroposon C $\gamma$  found in higher primates appears to be evolving neutrally and appears to have no function as a mature protein.

## Supporting Information

**Figure S1 Multiple sequence alignment of segment corresponding to exons 2–10 of human PKA C $\alpha$ 1 (*i.e.***

**residues 16–350).** All sequences are described in Materials and Methods S1. Residue numbering of human PKA C $\alpha$ 1 (identifier P17612) is shown above the sequence. Sequences belonging to the C $\alpha$ , C $\gamma$ , and C $\beta$  clades are marked at the right by a green, blue, and red bar, respectively. The figure was prepared with Jalview [44].

(PDF)

**Table S1 Sequence data for PKA catalytic subunit homologs from chordates collected and manipulated as described in Materials and Methods S1.**

(PDF)

**Materials and Methods S1 Details on sequence data collection.**

(PDF)

## Acknowledgments

We are grateful to Russell Orr and Kamran Shalchian-Tabrizi for help and useful comments and the University of Oslo Biportal for computational infrastructure.

## Author Contributions

Conceived and designed the experiments: KS TJ TR BSS JKL. Performed the experiments: KS JKL. Analyzed the data: KS TJ TR BSS JKL. Contributed reagents/materials/analysis tools: KS JKL. Wrote the paper: KS TJ TR BSS JKL.

## References

- Manning G, Whyte DB, Martinez R, Hunter T, Sudarsanam S (2002) The protein kinase complement of the human genome. *Science* 298: 1912–1934.
- Skålhegg BS, Taskén K (2000) Specificity in the cAMP/PKA signaling pathway. Differential expression, regulation, and subcellular localization of subunits of PKA. *Front Biosci* 5: D678–D693.
- Taylor SS, Yang J, Wu J, Haste NM, Radzio-Andzelm E, *et al.* (2004) PKA: a portrait of protein kinase dynamics. *Biochim Biophys Acta* 1697: 259–269.
- Krebs EG, Beavo JA (1979) Phosphorylation-dephosphorylation of enzymes. *Annu Rev Biochem* 48: 923–959.
- Kim C, Xuong NH, Taylor SS (2005) Crystal structure of a complex between the catalytic and regulatory (RI $\alpha$ ) subunits of PKA. *Science* 307: 690–696.
- Anand GS, Krishnamurthy S, Bishnoi T, Kornev A, Taylor SS, *et al.* (2010) Cyclic AMP- and (*R*<sub>p</sub>)-cAMPS-induced conformational changes in a complex of the catalytic and regulatory (RI $\alpha$ ) subunits of cyclic AMP-dependent protein kinase. *Mol Cell Proteomics* 9: 2225–2237.

7. Sjöberg TJ, Kornev AP, Taylor SS (2010) Dissecting the cAMP-inducible allosteric switch in protein kinase A RI $\alpha$ . *Protein Sci* 19: 1213–1221.
8. Taskén K, Skålhegg BS, Taskén KA, Solberg R, Knutsen HK, et al. (1997) Structure, function, and regulation of human cAMP-dependent protein kinases. *Adv Second Messenger Phosphoprotein Res* 31: 191–204.
9. Corbin JD, Keely SL, Park CR (1975) The distribution and dissociation of cyclic adenosine 3': 5'-monophosphate-dependent protein kinases in adipose, cardiac, and other tissues. *J Biol Chem* 250: 218–225.
10. Doskeland SO, Ogreid D (1981) Binding proteins for cyclic AMP in mammalian tissues. *Int J Biochem* 13: 1–19.
11. Dell'Acqua ML, Scott JD (1997) Protein kinase A anchoring. *J Biol Chem* 272: 12881–12884.
12. Beene DL, Scott JD (2007) A-kinase anchoring proteins take shape. *Curr Opin Cell Biol* 19: 192–198.
13. Colledge M, Scott JD (1999) AKAPs: from structure to function. *Trends Cell Biol* 9: 216–221.
14. Wang L, Sunahara RK, Krumins A, Perkins G, Crochiere ML, et al. (2001) Cloning and mitochondrial localization of full-length D-AKAP2, a protein kinase A anchoring protein. *Proc Natl Acad Sci U S A* 98: 3220–3225.
15. Taskén K, Aandahl EM (2004) Localized effects of cAMP mediated by distinct routes of protein kinase A. *Physiol Rev* 84: 137–167.
16. Jarnæss E, Taskén K (2007) Spatiotemporal control of cAMP signalling processes by anchored signalling complexes. *Biochem Soc Trans* 35: 931–937.
17. Beebe SJ, Øyen O, Sandberg M, Frøysa A, Hansson V, et al. (1990) Molecular cloning of a tissue-specific protein kinase (C $\gamma$ ) from human testis - representing a third isoform for the catalytic subunit of cAMP-dependent protein kinase. *Mol Endocrinol* 4: 465–475.
18. Schiebel K, Winkelmann M, Mertz A, Xu X, Page DC, et al. (1997) Abnormal XY interchange between a novel isolated protein kinase gene, *PRKY*, and its homologue, *PRKX*, accounts for one third of all (Y+XX) males and (Y-)XY females. *Hum Mol Genet* 6: 1985–1989.
19. Zimmermann B, Chiorini JA, Ma Y, Kotin RM, Herberg FW (1999) PrKX is a novel catalytic subunit of the cAMP-dependent protein kinase regulated by the regulatory subunit type I. *J Biol Chem* 274: 5370–5378.
20. Pearce LR, Komander D, Alessi DR (2010) The nuts and bolts of AGC protein kinases. *Nat Rev Mol Cell Biol* 11: 9–22.
21. Showers MO, Maurer RA (1988) Cloning of cDNA for the catalytic subunit of cAMP-dependent protein kinase. *Methods Enzymol* 159: 311–318.
22. San Agustín JT, Leszyk JD, Nuwaysir LM, Witman GB (1998) The catalytic subunit of the cAMP-dependent protein kinase of ovine sperm flagella has a unique amino-terminal sequence. *J Biol Chem* 273: 24874–24883.
23. Reinton N, Ørstavik S, Haugen TB, Jahnsen T, Taskén K, et al. (2000) A novel isoform of human cyclic 3',5'-adenosine monophosphate-dependent protein kinase, C $\alpha$ -s, localizes to sperm midpiece. *Biol Reprod* 63: 607–611.
24. San Agustín JT, Witman GB (2001) Differential expression of the C $\alpha$  and C $\alpha$ 1 isoforms of the catalytic subunit of cyclic 3',5'-adenosine monophosphate-dependent protein kinase in testicular cells. *Biol Reprod* 65: 151–164.
25. Desseyn JL, Burton KA, McKnight GS (2000) Expression of a nonmyristylated variant of the catalytic subunit of protein kinase A during male germ-cell development. *Proc Natl Acad Sci U S A* 97: 6433–6438.
26. Skålhegg BS, Huang Y, Su T, Idzerda RL, McKnight GS, et al. (2002) Mutation of the C $\alpha$  subunit of PKA leads to growth retardation and sperm dysfunction. *Mol Endocrinol* 16: 630–639.
27. Nolan MA, Babcock DF, Wennemuth G, Brown W, Burton KA et al. (2004) Sperm-specific protein kinase A catalytic subunit C $\alpha$ 2 orchestrates cAMP signaling for male fertility. *Proc Natl Acad Sci U S A* 101: 13483–13488.
28. Uhler MD, Chrivia JC, McKnight GS (1986) Evidence for a second isoform of the catalytic subunit of cAMP-dependent protein kinase. *J Biol Chem* 261: 15360–15363.
29. Wiemann S, Kinzel V, Pyerin W (1991) Isoform C $\beta$ 2, an unusual form of the bovine catalytic subunit of cAMP-dependent protein kinase. *J Biol Chem* 266: 5140–5146.
30. Guthrie CR, Skålhegg BS, McKnight GS (1997) Two novel brain-specific splice variants of the murine C $\beta$  gene of cAMP-dependent protein kinase. *J Biol Chem* 272: 29560–29565.
31. Ørstavik S, Reinton N, Frengen E, Langeland BT, Jahnsen T, et al. (2001) Identification of novel splice variants of the human catalytic subunit C $\beta$  of cAMP-dependent protein kinase. *Eur J Biochem* 268: 5066–5073.
32. Kvissel AK, Ørstavik S, Øistad P, Rootwelt T, Jahnsen T, et al. (2004) Induction of C $\beta$  splice variants and formation of novel forms of protein kinase A type II holoenzymes during retinoic acid-induced differentiation of human NT2 cells. *Cell Signal* 16: 577–587.
33. Funderud A, Henanger HH, Hafte TT, Amieux PS, Ørstavik S, et al. (2006) Identification, cloning and characterization of a novel 47 kDa murine PKA C subunit homologous to human and bovine C $\beta$ 2. *BMC Biochem* 7: 20.
34. Larsen AC, Kvissel AK, Hafte TT, Avellan CI, Eikvar S, et al. (2008) Inactive forms of the catalytic subunit of protein kinase A are expressed in the brain of higher primates. *FEBS J* 275: 250–262.
35. Reinton N, Haugen TB, Ørstavik S, Skålhegg BS, Hansson V, et al. (1998) The gene encoding the C $\gamma$  catalytic subunit of cAMP-dependent protein kinase is a transcribed retroposon. *Genomics* 49: 290–297.
36. Beebe SJ, Salomonsky P, Jahnsen T, Li Y (1992) The C $\gamma$  subunit is a unique isozyme of the cAMP-dependent protein kinase. *J Biol Chem* 267: 25505–25512.
37. Zhang W, Morris GZ, Beebe SJ (2004) Characterization of the cAMP-dependent protein kinase catalytic subunit C $\gamma$  expressed and purified from sf9 cells. *Protein Expr Purif* 35: 156–169.
38. Canaves JM, Taylor SS (2002) Classification and phylogenetic analysis of the cAMP-dependent protein kinase regulatory subunit family. *J Mol Evol* 54: 17–29.
39. The UniProt Consortium (2011) Ongoing and future developments at the Universal Protein Resource. *Nucleic Acids Res* 39: D214–D219.
40. Sayers EW, Barrett T, Benson DA, Bolton E, Bryant SH, et al. (2011) Database resources of the National Center for Biotechnology Information. *Nucleic Acids Res* 39: D38–D51.
41. Flicek P, Amode MR, Barrell D, Beal K, Brent S, et al. (2011) Ensembl 2011. *Nucleic Acids Res* 39: D800–D806.
42. Altschul SF, Gish W, Miller W, Myers EW, Lipman DJ (1990) Basic local alignment search tool. *J Mol Biol* 215: 403–410.
43. Edgar RC (2004) MUSCLE: multiple sequence alignment with high accuracy and high throughput. *Nucleic Acids Res* 32: 1792–1797.
44. Waterhouse AM, Procter JB, Martin DMA, Clamp M, Barton GJ (2009) Jalview Version 2 - a multiple sequence alignment editor and analysis workbench. *Bioinformatics* 25: 1189–1191.
45. Posada D, Crandall KA (1998) MODELTEST: testing the model of DNA substitution. *Bioinformatics* 14: 817–818.
46. Abascal F, Zardoya R, Posada D (2005) ProtTest: selection of best-fit models of protein evolution. *Bioinformatics* 21: 2104–2105.
47. Le SQ, Gascuel O (2008) An improved general amino acid replacement matrix. *Mol Biol Evol* 25: 1307–1320.
48. Jones DT, Taylor WR, Thornton JM (1992) The rapid generation of mutation data matrices from protein sequences. *Comput Appl Biosci* 8: 275–282.
49. Huelsenbeck JP, Ronquist F (2001) MRBAYES: Bayesian inference of phylogenetic trees. *Bioinformatics* 17: 754–755.
50. Ronquist F, Huelsenbeck JP (2003) MrBayes 3: Bayesian phylogenetic inference under mixed models. *Bioinformatics* 19: 1572–1574.
51. Guindon S, Dufayard JF, Lefort V, Anisimova M, Hordijk W et al. (2010) New algorithms and methods to estimate maximum-likelihood phylogenies: assessing the performance of PhyML 3.0. *Syst Biol* 59: 307–321.
52. Stamatakis A (2006) RAXML-VI-HPC: maximum likelihood-based phylogenetic analyses with thousands of taxa and mixed models. *Bioinformatics* 22: 2688–2690.
53. Huson DH, Richter DC, Rausch C, Dezulian T, Franz M, et al. (2007) Dendroscope: An interactive viewer for large phylogenetic trees. *BMC Bioinformatics* 8: 460.
54. Crooks GE, Hon G, Chandonia JM, Brenner SE (2004) WebLogo: a sequence logo generator. *Genome Res* 14: 1188–1190.
55. Wang D, Zhang Y, Zhang Z, Zhu J, Yu J (2010) KaKs\_Calculator 2.0: a toolkit incorporating gamma-series methods and sliding window strategies. *Genomics Proteomics Bioinformatics* 8: 77–80.
56. Thompson EE, Kornev AP, Kannan N, Kim C, Ten Eyck LF, et al. (2009) Comparative surface geometry of the protein kinase family. *Protein Sci* 18: 2016–2026.
57. Whelan S, Lio P, Goldman N (2001) Molecular phylogenetics: state-of-the-art methods for looking into the past. *Trends Genet* 17: 262–272.
58. Felsenstein J (2004) *Inferring Phylogenies*. Sunderland, MA: Sinauer Associates.
59. Jeffroy O, Brinkmann H, Delsuc F, Philippe H (2006) Phylogenomics: the beginning of incongruence? *Trends Genet* 22: 225–231.
60. Bergsten J (2005) A review of long-branch attraction. *Cladistics* 21: 163–193.
61. Delsuc F, Brinkmann H, Chourrout D, Philippe H (2006) Tunicates and not cephalochordates are the closest living relatives of vertebrates. *Nature* 439: 965–968.
62. Dehal P, Boore JL (2005) Two rounds of whole genome duplication in the ancestral vertebrate. *PLoS Biol* 3: e314.
63. Masanori K (2007) The 2R hypothesis: an update. *Curr Opin Immunol* 19: 547–552.
64. Putnam NH, Butts T, Ferrier DE, Furlong RF, Hellsten U, et al. (2008) The amphioxus genome and the evolution of the chordate karyotype. *Nature* 453: 1064–1071.
65. Kuraku S, Meyer A, Kuratani S (2009) Timing of genome duplications relative to the origin of the vertebrates: did cyclostomes diverge before or after? *Mol Biol Evol* 26: 47–59.
66. Van de Peer Y, Maere S, Meyer A (2009) The evolutionary significance of ancient genome duplications. *Nat Rev Genet* 10: 725–732.
67. Meyer A, Van de Peer Y (2005) From 2R to 3R: evidence for a fish-specific genome duplication (FSGD). *Bioessays* 27: 937–945.
68. Hurley IA, Mueller RL, Dunn KA, Schmidt EJ, Friedman M, et al. (2007) A new time-scale for ray-finned fish evolution. *Proc Biol Sci* 274: 489–498.
69. Bisbee CA, Baker MA, Wilson AC, Haji-Azimi I, Fischberg M (1977) Albumin phylogeny for clawed frogs (*Xenopus*). *Science* 195: 785–787.
70. Hellsten U, Harland RM, Gilchrist MJ, Hendrix D, Jurka J, et al. (2010) The genome of the Western clawed frog *Xenopus tropicalis*. *Science* 328: 633–636.
71. Savolainen P, Fitzsimmons C, Arvestad L, Andersson L, Lundberg J (2005) ESTs from brain and testis of White Leghorn and red junglefowl: annotation, bioinformatic classification of unknown transcripts and analysis of expression levels. *Cytogenet Genome Res* 111: 79–87.

72. Mikkelsen TS, Wakefield MJ, Aken B, Amemiya CT, Chang JL, et al. (2007) Genome of the marsupial *Monodelphis domestica* reveals innovation in non-coding sequences. *Nature* 447: 167–177.
73. Renfree MB, Papenfuss AT, Deakin JE, Lindsay J, Heider T, et al. (2011) Genome sequence of an Australian kangaroo, *Macropus eugenii*, provides insight into the evolution of mammalian reproduction and development. *Genome Biol* 12: R81.
74. Hurst LD (2002) The  $K_a/K_s$  ratio: diagnosing the form of sequence evolution. *Trends Genet* 18: 486.
75. Pink RC, Wicks K, Caley DP, Punch EK, Jacobs L, et al. (2011) Pseudogenes: pseudo-functional or key regulators in health and disease? *RNA* 17: 792–798.
76. Knighton DR, Zheng JH, Ten Eyck LF, Ashford VA, Xuong NH, et al. (1991) Crystal structure of the catalytic subunit of cyclic adenosine monophosphate-dependent protein kinase. *Science* 253: 407–414.
77. Breitenlechner C, Engh RA, Huber R, Kinzel V, Bossemeyer D, et al. (2004) The typically disordered N-terminus of PKA can fold as a helix and project the myristoylation site into solution. *Biochemistry* 43: 7743–7749.
78. Seifert MH, Breitenlechner CB, Bossemeyer D, Huber R, Holak TA, et al. (2002) Phosphorylation and flexibility of cyclic-AMP-dependent protein kinase (PKA) using  $^{31}\text{P}$  NMR spectroscopy. *Biochemistry* 41: 5968–5977.
79. Geselchen F, Bertinetti O, Herberg FW (2006) Analysis of posttranslational modifications exemplified using protein kinase A. *Biochim Biophys Acta* 1764: 1788–1800.
80. Torkamani A, Kannan N, Taylor SS, Schork NJ (2008) Congenital disease SNPs target lineage specific structural elements in protein kinases. *Proc Natl Acad Sci U S A* 105: 9011–9016.
81. Khavrutskii IV, Grant B, Taylor SS, McCammon JA (2009) A transition path ensemble study reveals a linchpin role for  $\text{Mg}^{2+}$  during rate-limiting ADP release from protein kinase A. *Biochemistry* 48: 11532–11545.
82. Yang J, Kennedy EJ, Wu J, Deal MS, Pennypacker J, et al. (2009) Contribution of non-catalytic core residues to activity and regulation in protein kinase A. *J Biol Chem* 284: 6241–6248.
83. Kornev AP, Haste NM, Taylor SS, Eyck LF (2006) Surface comparison of active and inactive protein kinases identifies a conserved activation mechanism. *Proc Natl Acad Sci U S A* 103: 17783–17788.
84. Badrinarayan P, Sastry GN (2011) Sequence, structure, and active site analyses of p38 MAP kinase: exploiting DFG-out conformation as a strategy to design new type II leads. *J Chem Inf Model* 51: 115–129.
85. Taylor SS, Kim C, Cheng CY, Brown SH, Wu J, et al. (2008) Signaling through cAMP and cAMP-dependent protein kinase: diverse strategies for drug design. *Biochim Biophys Acta* 1784: 16–26.
86. Wu J, Brown SH, von Daake S, Taylor SS (2007) PKA type II $\alpha$  holoenzyme reveals a combinatorial strategy for isoform diversity. *Science* 318: 274–279.
87. Niedner RH, Buzko OV, Haste NM, Taylor A, Gribskov M, et al. (2006) Protein kinase resource: an integrated environment for phosphorylation research. *Proteins* 63: 78–86.
88. Hanks SK, Hunter T (1995) Protein kinases 6. The eukaryotic protein kinase superfamily: kinase (catalytic) domain structure and classification. *FASEB J* 9: 576–596.
89. Goldman N, Yang Z (1994) A codon-based model of nucleotide substitution for protein-coding DNA sequences. *Mol Biol Evol* 11: 725–736.
90. Zhang Z, Li J, Zhao XQ, Wang J, Wong GKS, et al. (2006) KaKs\_Calculator: calculating  $K_a$  and  $K_s$  through model selection and model averaging. *Genomics Proteomics Bioinformatics* 4: 259–263.